

## Transverse Enhancement, Longitudinal Quenching and Coulomb Sum Rule in $e^{-12}\text{C}$ and $e^{-16}\text{O}$ Scattering

---

A. Bodek<sup>a,\*</sup> and M. E. Christy<sup>b</sup>

<sup>a</sup>*Department of Physics and Astronomy, University of Rochester,  
Rochester, NY 14627, USA*

<sup>b</sup>*Thomas Jefferson National Accelerator Facility,  
Newport News, VA 23606, USA*

*E-mail:* [bodek@pas.rochester.edu](mailto:bodek@pas.rochester.edu), [christy@jlab.org](mailto:christy@jlab.org)

We present a short summary of a phenomenological analysis of all available electron scattering data on  $^{12}\text{C}$  (about 6600 differential cross section measurements) and on  $^{16}\text{O}$  (about 250 measurements) within the framework of the quasielastic superscaling model (including Pauli blocking). All quasielastic and inelastic cross section measurements are included down to the lowest momentum transfer  $\mathbf{q}$  (including photo-production data). We find that there is enhancement of the transverse quasielastic response function and quenching of the longitudinal response function at low  $\mathbf{q}$  (in addition to Pauli blocking). We extract parameterizations of a *multiplicative* low  $\mathbf{q}$  "Longitudinal Quenching Factor" and an *additive* "Transverse Enhancement" contribution. Additionally, we find that the excitation of nuclear states contribute significantly (up to 30%) to the Coulomb Sum Rule. We extract the most accurate determination of the sum rule to date and find it to be in disagreement with random phase approximation based calculations but in reasonable agreement with recent theoretical calculations such as "First Principle Green's Function Monte Carlo".

*41st International Conference on High Energy physics - ICHEP2022  
6-13 July, 2022  
Bologna, Italy*

---

\*Speaker

We present a short summary of results reported in [1] on a fit to all available electron scattering data on  $^{12}\text{C}$  (about 6600 differential cross section measurements) and  $^{16}\text{O}$  (about 250 measurements) within the framework of the quasielastic (QE) superscaling model (including Pauli blocking). The cross sections measurements include the available data on QE (down to the lowest momentum transfer  $\mathbf{q}$  ( $\equiv |\vec{q}|$ )), inelastic production, and photoproduction. The fit includes inelastic structure functions and empirical parameters to model both an enhancement of the transverse QE response function  $R_T^{QE}$  and quenching of the longitudinal response function  $R_L^{QE}$  at low  $\mathbf{q}$ . As the fit provides an accurate description of the data, it can be used as a proxy to validate modeling of cross sections in Monte Carlo event generators for electron and neutrino ( $\nu_{e,\mu}$ ) scattering. The "Transverse Enhancement"  $\text{TE}(\mathbf{q}, \nu)$  of  $R_T^{QE}$  and the "Quenching Factor"  $F_{quench}^L(\mathbf{q})$  of  $R_L^{QE}$  are of great interest to  $\nu_{e,\mu}$  scattering experiments. The electron scattering differential cross section can be written as

$$\frac{d^2\sigma}{d\nu d\Omega} = \sigma_M [AR_L(\mathbf{q}, \nu) + BR_T(\mathbf{q}, \nu)], \quad \sigma_M = \alpha^2 \cos^2(\theta/2) / [4E_0^2 \sin^4(\theta/2)]$$

Here,  $E_0$  is the incident electron energy,  $E'$  and  $\theta$  are energy and angle of the final state electron,  $\nu = E_0 - E'$ ,  $Q^2$  is the square of the 4-momentum transfer (defined to be positive),  $\mathbf{q}^2 = Q^2 + \nu^2$ ,  $A = (Q^2/\mathbf{q}^2)^2$  and  $B = \tan^2(\theta/2) + Q^2/2\mathbf{q}^2$ . In the analysis we also use the invariant hadronic mass  $W^2 = M_p^2 + 2M_p\nu - Q^2$ .

The inelastic Coulomb Sum Rule is the integral of  $R_L(\mathbf{q}, \nu)d\nu$ , *excluding the elastic peak and pion production processes*. It has contributions from QE scattering and from electro-excitations of nuclear states. Dividing by the square of the proton electric form factor  $G_{Ep}$  we obtain the normalized inelastic Coulomb Sum Rule  $SL(\mathbf{q})$ . Careful consideration of nuclear excitations is critical for an accurate extraction of the normalized Coulomb Sum Rule  $SL(\mathbf{q})$  at low  $\mathbf{q}$  as these states can contribute up to 30%. At high  $\mathbf{q}$  it is expected that  $S_L \rightarrow 1$  because both nuclear excitation form factors and Pauli suppression are small. At small  $\mathbf{q}$  it is expected that  $S_L \rightarrow 0$  because form factors for all nuclear excitations must be zero at  $\mathbf{q}=0$ .

In addition to performing a universal fit to all  $^{12}\text{C}$  and  $^{16}\text{O}$  electron scattering data we also parameterize the measurements of the L and T form factors for the electro-excitation of all nuclear states in with excitation energies ( $E_x$ ) less than 50.0 MeV. The contributions of nuclear excitation to  $SL(\mathbf{q})$  are calculated using the parametrizations of the form factors. The bottom two panels of Fig. 1 show the contributions of nuclear excitations to  $SL(\mathbf{q})$  for  $^{12}\text{C}$  and  $^{16}\text{O}$ . The contribution of all excitations is largest ( $\approx 0.29$ ) at  $\mathbf{q}=0.22$  GeV. Although the contributions of different  $E_x$  regions to  $SL(\mathbf{q})$  is different for  $^{12}\text{C}$  and  $^{16}\text{O}$ , the total contribution turns out to be similar for the two nuclei. The top two panels of Fig. 1 show comparisons of our fit to some of the  $R_L$  measurements by Yamaguchi 1996[2]. The universal fit to the  $^{12}\text{C}$  data is an update of the 2012 fit by Bosted and Mamyan[3]. The QE contribution is modeled by the superscaling approach with Pauli blocking calculated using the Rosenfelder method. The superscaling function extracted from the fit is similar to the superscaling functions of Amaro et al.[4] and yields similar Pauli suppression. In modeling the QE response we use the same scaling function for both  $R_L^{QE}(\mathbf{q}, \nu)$  and  $R_T^{QE}(\mathbf{q}, \nu)$  and fit for empirical corrections to the response functions. For  $R_T^{QE}$  we extract an *additive* "Transverse Enhancement/MEC"  $\text{TE}(\mathbf{q}, \nu)$  contribution (which includes both single nucleon and two nucleon final states).  $\text{TE}(\mathbf{q}, \nu)$  increases  $R_T^{QE}$  with the largest fractional contribution around  $Q^2=0.3$  GeV $^2$ .

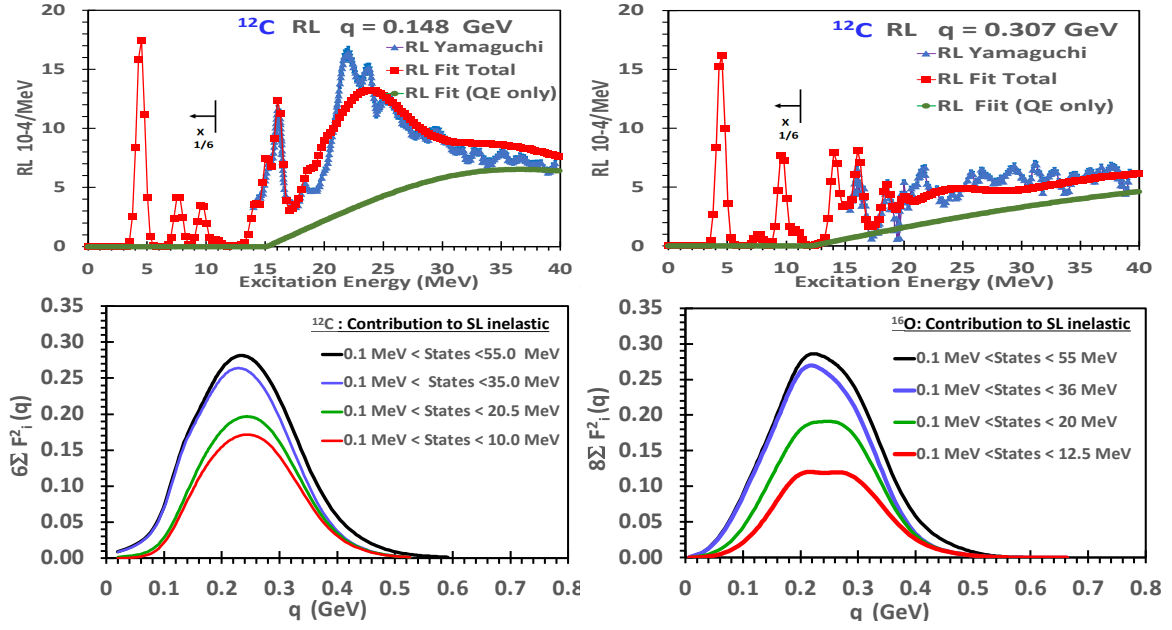


**Figure 1:** Top two panels: Comparison of  $R_L(\mathbf{q}, \nu)$  extracted from our  $^{12}\text{C}$  fit to a sample of experimental data. For excitation energies  $< 12 \text{ MeV}$  the values are multiplied by  $1/6$ . Bottom two panels: The contributions of longitudinal nuclear excitations (between 2 and 55 MeV) to the Coulomb sum rule for  $^{12}\text{C}$  and  $^{16}\text{O}$ .

For  $R_L^{QE}$  we extract a *multiplicative*  $\mathbf{q}$  dependent "Longitudinal Quenching Factor",  $F_{quench}(\mathbf{q})$ , which decreases  $R_L^{QE}$  at low  $\mathbf{q}$ .

Since  $\frac{d^2\sigma}{d\Omega d\nu}$  measurements span a range of  $\theta$  and  $\mathbf{q}$ , parametrizations of both  $\text{TE}(\mathbf{q}, \nu)$  and  $F_{quench}^L(\mathbf{q})$  can be extracted. The analysis includes all data for a range of nuclei. However, in this paper we only include electron scattering data on  $^1\text{H}$ ,  $^2\text{H}$ ,  $^{12}\text{C}$  and  $^{16}\text{O}$ . Briefly, the fit includes:

1. Coulomb corrections using the Effective Momentum Approximation (EMA) in modeling scattering from nuclear targets.
2. Updated nuclear elastic+excitations form factors.
3. Superscaling  $FN(\psi')$  parameters re-extracted including the broadening parameter  $K_F$ .
4. Parameterizations of the free nucleon form factors re-derived from all  $^1\text{H}$  and  $^2\text{H}$  data.
5. Rosenfelder Pauli suppression which reduces and changes the QE distribution at low  $\mathbf{q}$  and  $\nu$ .
6. Updates of fits to inelastic electron scattering data (in the nucleon resonance region and inelastic continuum) for  $^1\text{H}$  and  $^2\text{H}$ .
7. A  $\mathbf{q}$  dependent  $E_{\text{shift}}^{QE}(\mathbf{q})$  parameter accounting for the optical potential of final state nucleons.
8. Photo-production data in the nucleon resonance region and inelastic continuum.
9. Gaussian Fermi smeared nucleon resonance and inelastic continuum. The  $K_F$  parameters for pion production and QE can be different.

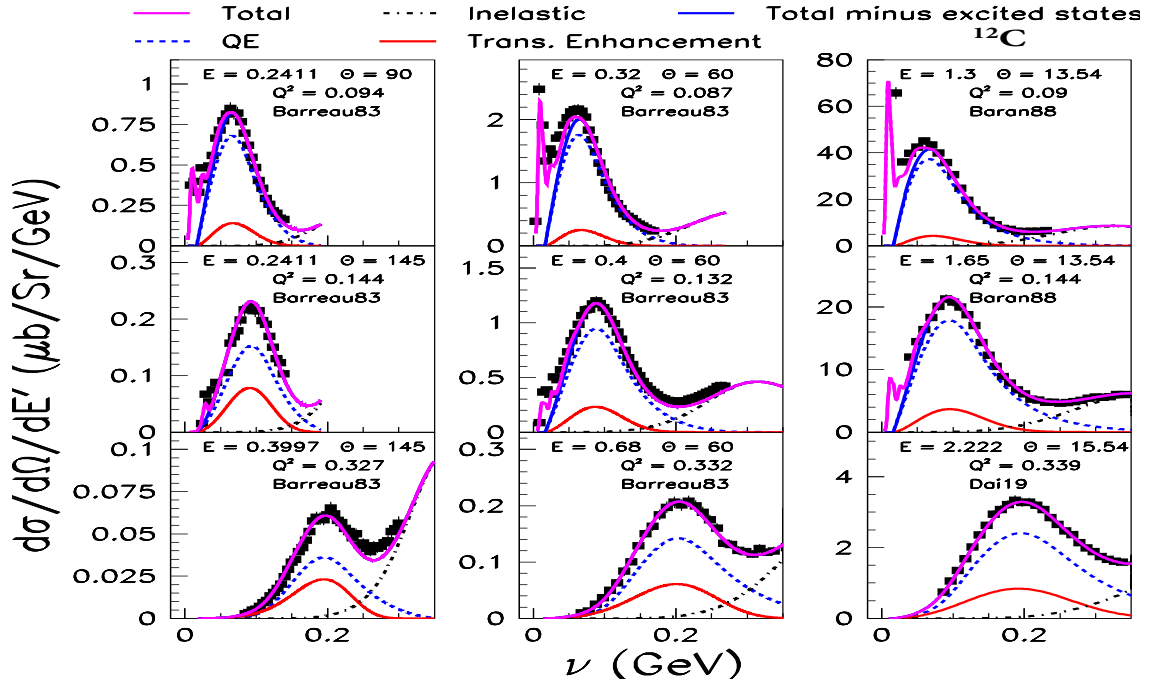


**Figure 2:** Comparison of the fit to electron scattering  $\frac{d^2\sigma}{d\Omega d\nu}$  measurements at  $\mathbf{q}$  values close to 0.30, 0.38 and 0.57 GeV (and different scattering angles). Total  $\frac{d^2\sigma}{d\Omega d\nu}$  (solid-purple line), total minus the contribution of the nuclear excitations (solid-blue), the QE cross section without TE (dashed-blue), the TE( $\mathbf{q}, \nu$ ) contribution (solid-red) and inelastic pion production (dot-dashed black line) are shown.

10. Parametrizations of the medium modifications of both the L and T structure functions responsible for the EMC effect (nuclear dependence of inelastic structure functions). These are applied to the free nucleon cross sections prior to application of the Fermi smearing.
11. Parametrizations of TE( $\mathbf{q}, \nu$ ) and  $F_{quench}^L(\mathbf{q})$  as described below.
12. QE data at *all values* of  $Q^2$  down to  $Q^2=0.01$  GeV<sup>2</sup> ( $\mathbf{q}=0.1$  GeV) (which were not included in the Bosted-Mamyan fit).

The average (over  $\nu$ ) Pauli blocking factor for  $x < 2.5$  ( $x = \mathbf{q}/K_F$ ,  $K_F=0.228$  GeV) is given by:

$$\langle F_{Pauli}^{This-analysis}(\mathbf{q}) \rangle = \sum_{j=0}^{j=3} k_j(x)^j. \quad (1)$$

For the superscaling function used in this analysis  $k_0=0.3054$ ,  $k_1=0.7647$ ,  $k_2=-0.2768$  and  $k_3=0.0328$ . The Pauli suppression factor for  $x > 2.5$  is 1.0.

Comparisons of the fit to electron scattering  $\frac{d^2\sigma}{d\Omega d\nu}$  measurements at different values of  $\theta$  for  $\mathbf{q}$  values close to 0.30, 0.38 and 0.57 GeV (corresponding to extractions of  $R_L$  and  $R_T$  by Jourdan[6]) are shown in Fig. 2. Shown are the total  $\frac{d^2\sigma}{d\Omega d\nu}$  cross section (solid-purple line), the total minus the contribution of nuclear excitations (solid-blue), the QE cross section without TE (dashed-blue), the TE contribution (solid-red), and inelastic pion production (dot-dashed black). The fit is in good agreement with all electron scattering data for both small and large  $\theta$ .

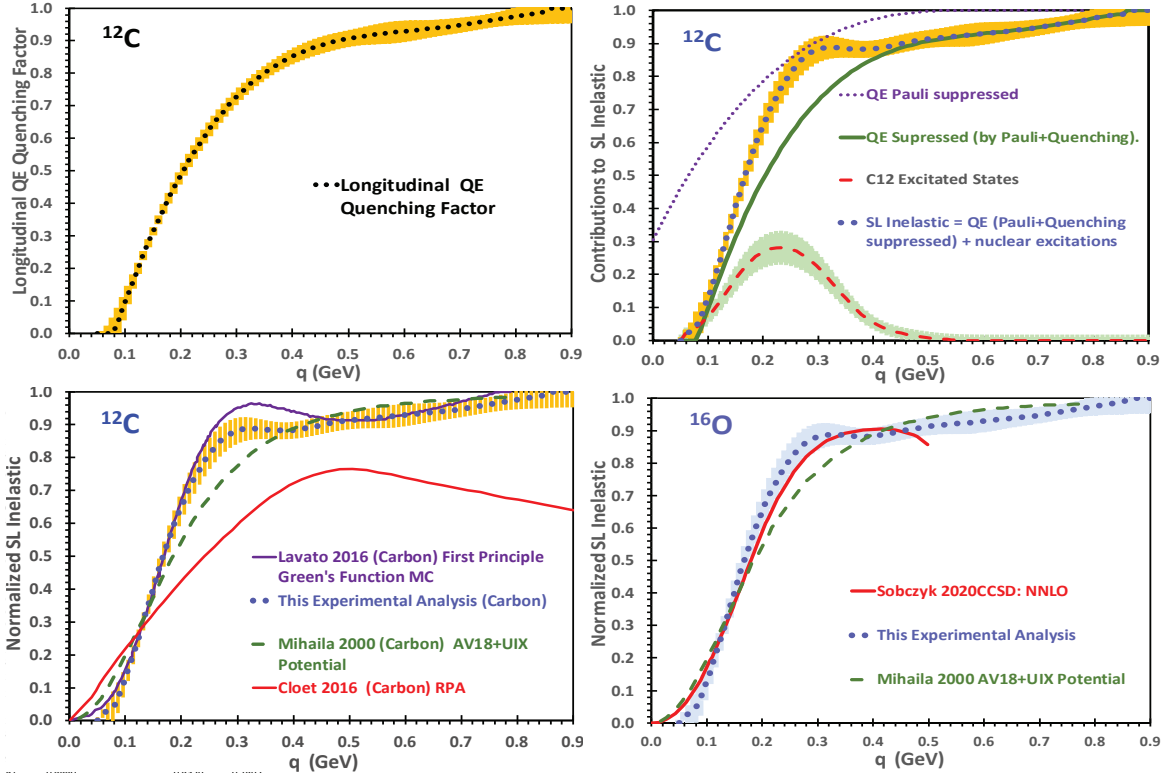


**Figure 3:** Top left panel: QE "Longitudinal Quenching Factor" (dotted-black line with yellow error band). Top right panel: The various contributions to  $SL(\mathbf{q})$  for  $^{12}\text{C}$  (dotted blue with yellow error band) including QE with Pauli suppression only (dotted-purple), QE suppressed by both "Pauli" and "Longitudinal Quenching" (solid-green), and the contribution of nuclear excitations (red-dashed with green error band). Bottom left panel:  $SL(\mathbf{q})$  for  $^{12}\text{C}$  (dotted-blue with yellow error band) compared to theoretical calculations including Lovato 2016 (solid-purple), Mihaila 2000 (dashed-green), and RPA Cloet 2016 (solid-red). Bottom right panel:  $SL(\mathbf{q})$  for  $^{16}\text{O}$  (dotted-black with green error band) compared to theoretical calculations of Sobczyk 2020 (red-dashed) and Mihaila 2000 (dotted-dashed).

The extracted QE "Longitudinal Quenching Factor"  $F_{quench}^L(\mathbf{q})$  is unity for  $x > 3.75$ , and is zero for  $x < 0.35$ . For  $0.35 < x < 4.0$  it is parameterized by:

$$F_{quench}^L(\mathbf{q}) = \frac{(x - 0.2)^2}{(x - 0.18)^2} \left[ 1.0 + A_1(3.75 - x)^{1.5} + A_2(3.75 - x)^{2.5} + A_3(3.75 - x)^{3.5} \right] \quad (2)$$

with  $A_1 = -0.13152$ ,  $A_2 = 0.11693$ , and  $A_3 = -0.03675$ . The top-left panel of Fig. 3 shows the extracted  $F_{quench}^L(\mathbf{q})$ . (black-dotted line). The yellow band includes the statistical, parameterization and a normalization error of 2% (all added in quadrature).

If another formalism is used to model QE scattering (e.g. RFG or spectral functions) then the quenching factor for the model  $F_{quench}^{model}(\mathbf{q})$  is given by:

$$F_{quench}^{L-model}(\mathbf{q}) = \frac{\langle F_{Pauli}^{This-analysis}(\mathbf{q}) \rangle}{\langle F_{Pauli}^{model}(\mathbf{q}) \rangle} F_{quench}^L(\mathbf{q}) \quad (3)$$

The top right panel of Fig. 3 shows the various contributions to the measured  $SL(\mathbf{q})$  for  $^{12}\text{C}$  (dotted blue line with yellow error band). Shown are the QE contribution with only Pauli suppression

(dotted-purple), QE suppressed by both "Pauli Suppression" and  $F_{quench}^L(\mathbf{q})$  labeled as QE total suppression (solid-green), and the contribution of nuclear excitations (red-dashed line). The green error band is 15% plus 0.01 added in quadrature.

The left panel on the bottom of Figure 3 shows a comparison of the extracted  $SL(\mathbf{q})$  for  $^{12}\text{C}$  (dotted-blue curve with yellow error band) to theoretical calculations (by Lovato, Mihaila, Cloet and Sobczyk)[5]. Lovato 2016 is a "First Principle Green's Function Monte Carlo" (GFMC)(solid-purple line), Mihaila 2000 is a Coupled-Clusters calculation (AV18+UIX potential, dashed-green) and Cloet 2016 is based on RPA (solid-red). Our measurement for  $^{12}\text{C}$  are in disagreement with Cloet 2016 RPA, and in reasonable agreement with Lovato 2016 and Mihaila 2000 except near  $\mathbf{q} \approx 0.30$  GeV where the contribution from nuclear excitations is significant.

The bottom right panel of Fig. 3 shows  $SL(\mathbf{q})$  for  $^{16}\text{O}$  (dotted-blue with green error band) compared to theoretical calculations [5] by Sobczyk 2020 ("Coupled-Cluster with Singles-and Doubles NNLO<sub>sat</sub>", red-dashed line), and Mihaila 2000 (Coupled-Cluster calculation with (AV18+UIX potential, dashed green line). The data are in reasonable agreement with Sobczyk 2020 and Mihaila 2000 calculations for  $^{16}\text{O}$  except near  $\mathbf{q} \approx 0.30$  GeV where the contribution from nuclear excitations is significant.

The  $TE(\mathbf{q}, \nu)$  contribution to the QE transverse structure function  $F_1(Q^2, \nu)$  for  $^{12}\text{C}$  is parameterized as a distorted Gaussian centered around  $W \approx 0.88$  GeV and a Gaussian at  $W \approx 1.2$  GeV with  $Q^2$  dependent width and amplitude.  $F_1^{MEC}=0$  for  $\nu < \nu_{min}$  ( $\nu_{min}=16.5$  MeV). For  $\nu > \nu_{min}$  it is given by  $F_1^{MEC} = \max((f_1^A + f_1^B), 0.0)$  where

$$\begin{aligned} f_1^A &= a_1 Y \cdot [(W^2 - W_{min}^2)^{1.5} \cdot e^{-(W^2 - b_1)^2 / 2c_1^2}] \\ f_1^B &= a_2 Y \cdot (Q^2 + q_0^2)^{1.5} \cdot [e^{-(W^2 - b_2)^2 / 2c_2^2}] \\ Y &= A e^{-Q^4 / 12.715} \frac{(Q^2 + q_0^2)^2}{(0.13380 + Q^2)^{6.90679}} \\ a_1 &= 0.091648, \quad a_2 = 0.10223, \quad W_{min}^2 = M_p^2 + 2M_p \nu_{min} - Q^2 \end{aligned}$$

where  $Q^2$  is in units of  $\text{GeV}^2$ ,  $M_p$  is the proton mass,  $A$  is the atomic weight,  $q_0^2 = 1.0 \times 10^{-4}$ ,  $b_1 = 0.77023$ ,  $c_1 = 0.077051 + 0.26795Q^2$ ,  $b_2 = 1.275$ , and  $c_2 = 0.375$ .

This Research is supported by the U.S. Department of Energy, Office of Science, under grant DE-SC0008475, and contract DE-AC05-06OR23177.

## References

- [1] A. Bodek and M. E. Christy, arXiv:2208.14772 (2022),
- [2] Y. Yamaguchi et al. Phys. Rev. D3, 1750 (1971).
- [3] P.E. Bosted and V. Mamyan, arXiv:1203.2262 (2012).
- [4] J. E. Amaro et al. Phys. Rev. C 71, 015501 (2005); J. E. Amaro et al. J. Phys. G: Nucl. Part. Phys. 47, 124001 (2020).
- [5] A. Lovato et al., Phys. Rev. Lett. 117, 082501 (2016); B. Mihaila and J. H. Heisenberg, Phys. Rev. Lett. 84 (2000) 1403; J. E. Sobczyk et al., Phys.Rev.C 102 (2020) 064312; I. Cloet et al. (RPA) Phys. Rev. Lett. 116, 032701 (2016).
- [6] J. Jourdan, Nucl. Phys. A603, 117 (1996); J. Jourdan, Phys. Lett. B353, 189 (1995).